A Time-Average Model of the RF Plasma Sheath

Demetre J. Economou*[,1]

Department of Chemical Engineering, University of Illinois, Urbana, Illinois 61801

David R. Evans*

Tektronix Incorporated, Beaverton, Oregon 97077

Richard C. Alkire*

Department of Chemical Engineering, University of Illinois, Urbana, Illinois 61801

ABSTRACT

A time-average model of the RF plasma sheath was developed. The ion "fluid" equations were used with a frictional force to account for ion-neutral collisions. Consideration of the collision dynamics showed that the frictional force may be taken as proportional to the square of the ion drift velocity. The sheath model was used to investigate the ion energy and flux on the electrodes of plasma reactors. The dimensionless quantity Co (collision number) was found to be important in describing the ion motion in the sheath. An analytical expression for the ion bombardment energy was derived, in terms of Co and the sheath voltage, for the range of parameter values typical of high pressure (~1 torr) diode plasma etchers. An application of the model to an oxygen discharge in a parallel plate reactor was considered. Over the parameter range investigated, the ion bombardment energy was found to be only a few tens of eV, much lower than typical sheath voltages (~200V). The ion bombardment energy was found to be a function of the sheath electric-field-to-pressure ratio. The model provides a framework that can be incorporated into more general plasma reactor models which consider transport and reaction phenomena along surfaces undergoing etching.

Within the last decade, dry etching using an RF diode discharge in a chemically reactive gas has become a widespread technique in the fabrication of microelectronic devices. Under conditions of relatively high pressure (~1 torr) and high frequency (~10 MHz), an RF discharge of this kind may resemble an ideal, nonequilibrium, slightly ionized plasma separated from wall and electrode surfaces by a region of positive space charge or sheath. In the sheath region ions are accelerated toward electrode or wall surfaces by the electric field present due to the space charge. In their transit through the sheath, ions may experience collisions, mainly with neutrals owing to the low degree of ionization ($\leq 10^{-4}$). Such collisions serve to reduce the energy and randomize the ionic motion. Determination of the ion flux and the energy and angular distribution functions of ions striking the electrodes of plasma reactors is of significant technological interest in semiconductor processing. Such quantities affect both the etching rate and the degree of anisotropy in plasma etching applications. The purpose of this paper is to develop an approximate model to investigate the behavior of ionic species within the high field sheath regions of a gas discharge.

Quantities that affect the energy and/or directionality of bombarding ions include the sheath electric-field-to-pressure ratio (E/p) (1, 2), the applied frequency (3), and the nature and topography of the surface (4, 5). The quantity E/p is a measure of the energy imparted to an ion by the electric field over the distance of one mean free path. Frequency has a pronounced effect on ion bombardment energy. At low frequencies ions can respond to the instantaneous sheath voltage and, in the absence of collisions, the maximum ion energy would correspond to the peak sheath voltage. At high frequencies, ions respond to a time-average sheath potential. The transition from low to high frequency regime happens at about 1 MHz (3, 6). The present study emphasizes applications at 13.56 MHz. Hence ions can be regarded as responding to an average sheath voltage (7), so that an equivalent dc model of the RF sheath may be applied. Further, if the sheath is thick compared to the ion mean free path, the ion bombarding energy would lie well below the average sheath voltage. However, if the sheath thickness is comparable to the mean free path, the ion energy would extend close to the average sheath voltage.

A rigorous approach to solving for the particle transport in the sheath would require consideration of Boltzmann-like kinetic equations for the ions, electrons, and neutrals, coupled to the Poisson equation for the self-consistent electric field. Solution of the coupled integro-differential equations subject to appropriate boundary conditions could yield the corresponding distribution functions. Such an approach is invariably difficult, although progress has recently been made in solving for the spatially dependent energy distribution functions of ions, electrons, and fast neutrals (resulting from charge exchange collisions) in a time-independent sheath (8). Another approach is to employ the Monte Carlo method as demonstrated by Kushner (9). A simplified approach was taken in the present study motivated by the fact that a reasonable sheath model be developed, yet simple enough to be readily incorporated into a more general plasma reactor model. Thus, in the present sheath model, the ion "fluid" velocity was found by coupling the equations of continuity and motion of the ion "cloud" to Poisson's equation for the potential distribution in the sheath. Time-averaged quantities were used throughout, *i.e.* an equivalent dc model was employed. Equivalent dc models of RF sheaths have been used before (10). Their advantage is the simplicity of the calculation. Their disadvantage is that they are not applicable to low frequency (<10 MHz) operation and that they provide only the average ion energy and not the ion energy distribution.

Model Formulation

To eliminate edge effects and to reduce the dimensionality of the analysis, the sheath shall be considered as an infinite planar sheet of finite thickness between an infinite planar absorbing surface and a semi-infinite plasma. Within the sheath the medium shall be regarded as two interpenetrating fluids composed of neutral gas molecules and singly charged daughter ions, respectively. In all cases, the neutral fluid will be taken to be in thermal equilibrium at some ambient temperature, T. The ions and the neutrals are of equal mass, m. The electron density will be taken to be negligible since the sheath is a region of positive space charge (*i.e.*, deficient in electrons). If one further assumes the absence of temperature gradients and strong magnetic fields, the behavior of the ion fluid can be described by three coupled differential equations

$$\frac{\partial n_i}{\partial t} + \frac{\partial}{\partial x}(n_i u_i) = 0 \quad [1]$$

*Electrochemical Society Active Member.

[1]Present address: Department of Chemical Engineering, University of Houston, Houston, Texas 77004.

$$\frac{\partial u_i}{\partial t} + u_i \frac{\partial u_i}{\partial x} = \frac{qE}{m} + \frac{F_i}{m} \quad [2]$$

$$\frac{\partial E}{\partial x} = \frac{q n_i}{\epsilon_o} \quad [3]$$

Here, the coordinate x is in the direction normal to the planar boundary surfaces defined previously. Equation [1] is the ion continuity equation. It contains no source term and, thus, embodies the assumption that the ionization rate is negligible within the sheath in comparison to the plasma or glow region. This assumption is consistent with the assumption of negligible electron density since electron impact is usually the dominant ionization mechanism. Equation [2] is the equation of motion for the ion fluid with u_i denoting the average ion velocity. The two terms on the right-hand side account, respectively, for the effect of the sheath electric field and the effect of the dynamic frictional force, F_i, due to interaction with the medium. Equation [3] is Poisson's equation which relates the divergence of the electric field to the space charge density.

Dynamic friction.—The preceding set of equations is closed in all quantities except the frictional force, F_i. In this section, a form for F_i as a function of molecular dynamic parameters and the average ion velocity, u_i, will be obtained. To begin, one notes that within a slightly ionized discharge, the great majority of collisions experienced by any given ion are binary encounters with a neutral gas molecule (shown schematically in Fig. 1). Phenomenologically, one can express the dynamic frictional force as an average over all possible collisions of a "test" ion moving at a velocity, u_i, with a thermal distribution of neutrals. Restriction of consideration to spherically symmetric ion-molecule interactions yields the expression

$$F_i - \frac{m}{2} \int_0^\pi d\chi \sin\chi \int d\mathbf{g}\, g\sigma(\chi, g)\, \Delta u_i(\chi, \mathbf{g}) f(\mathbf{v}) \quad [4]$$

where $\mathbf{g}$ is the relative velocity of the test ion with respect to a gas molecule ($g = |\mathbf{g}|$) and χ is the collisional scattering angle (see Fig. 1). The function, $\sigma(\chi, g)$, is the differential collision cross section for the ion-molecule interaction and $\Delta u_i(\chi, \mathbf{g})$ is the collisional change in the component of the ion velocity parallel to the X-axis (*i.e.*, normal to electrode or wall surfaces). The molecular velocity distribution function, $f(\mathbf{v})$, is taken to be a Maxwellian

$$f(\mathbf{v}) = N \left[\frac{m}{2\pi kT}\right]^{3/2} e^{-mv^2/2kT} \quad [5]$$

where the molecular velocity magnitude, v, is

$$v = \sqrt{g^2 - 2gu_i \cos\theta + u_i^2} \quad [6]$$

and the angle θ is taken between the relative velocity $\mathbf{g}$ and the X-axis.

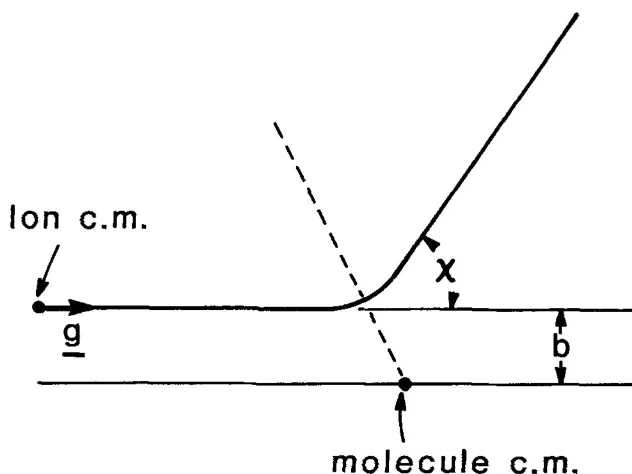

Fig. 1. Ion-molecule collision geometry

For mathematical convenience, the differential collision cross section will be assumed to be independent of g [*i.e.*, $\sigma(\chi, g) = \sigma(\chi)$] and $\Delta u_i(\chi, \mathbf{g})$ will be assumed to be of the form

$$\Delta u_i(\chi, \mathbf{g}) = -g \cos\theta\, \xi(\chi) \quad [7]$$

Physically, this corresponds to a hard sphere description of the ion-molecule interaction. Such a description is plausible since the collisional kinetic energy is generally quite large and the repulsive core of the interaction is dominant. Of course, a hard sphere interaction neglects the energy dependence of the cross section. Conceptually, the use of a "soft" interaction (such as a Lennard-Jones 6-12 potential) would present no difficulty except for more laborious computations. However, the value of such increased sophistication is questionable since (*i*) F_i is an integral quantity and is not strongly dependent on the detailed nature of the interaction, and (*ii*) in the approximate sheath model, the ion energy distribution is replaced by the average ion energy.

One can substitute Eq. [5]-[7] into the expression for F_i Eq. [4], and integrate to obtain

$$F_i = -\frac{mN}{\pi u_i^2}\left[\frac{2\pi kT}{m}\right]^{3/2} \left\{ u_i e^{-mu^2_i/2kT}\left(1 - \frac{mu_i^2}{kT}\right) + \left[\left(\frac{mu_i^2}{kT}\right)^2 + \frac{2mu_i^2}{kT} - 1\right]\frac{1}{2}\sqrt{\frac{2\pi kT}{m}}\ \mathrm{erf}\left(u_i\sqrt{\frac{m}{2kT}}\right)\right\} \int_0^\pi d\chi \sin\chi\sigma(\chi)\xi(\chi) \quad [8]$$

In the present case, ions have kinetic energies which are much larger than kT, hence, the preceding expression can be simplified by the assumption $mu_i^2 >> 2kT$

$$F_i = -2\pi\, mNu_i^2 \int_0^\pi d\chi \sin\chi\sigma(\chi)\xi(\chi) \quad [9]$$

Thus, the frictional force is approximately quadratic in u_i. It is convenient to define a frictional coefficient, α_i, such that

$$F_i = -\alpha_i u_i^2 \quad [10]$$

where

$$\alpha_i = 2\pi\, mN \int_0^\pi d\chi \sin\chi\sigma(\chi)\xi(\chi) \quad [11]$$

The coefficient can be evaluated if specific forms are given for $\sigma(\chi)$ and $\xi(\chi)$. For elastic hard sphere interactions

$$\sigma_{el}(\chi) = \pi D^2 \quad [12]$$

$$\xi(\chi) = \frac{1}{2}(1 - \cos\chi) \quad [13]$$

Then, the frictional coefficient takes the form

$$\alpha_i = \frac{\pi\, mN\, D^2}{2} \quad [14]$$

Charge exchange collisions can be treated as grazing encounters which, if there were no charge exchange, would have a scattering angle near 0. However the effect of the charge exchange is to change the scattering angle to near π radians (for equal ion and neutral masses). If the constant, D_{ex}, is defined as an effective diameter appropriate to charge exchange, the charge exchange cross section can be given an idealized form

$$\sigma_{ex}(\chi) = \pi D_{ex}^2 \frac{\delta(\pi - \chi)}{\sin\chi} \quad [15]$$

where $\delta(\pi - \chi)$ is the Dirac delta function. Dynamically, all charge exchange collisions are being treated as if $\chi = \pi$.

The differential cross section including both elastic and charge exchange collisions is $\sigma_t = \sigma_{el} + \sigma_{ex}$. The form of $\xi(\chi)$ remains as in Eq. [13]. When charge exchange is included, α_i becomes

$$\alpha_i = \frac{Nm\pi}{2}(D^2 + D_{ex}^2) \qquad [16]$$

which suggests that an *ad hoc* general expression for α_i can be given as

$$\alpha_i = \frac{Nm}{2}\sigma_t \qquad [17]$$

Model equations and boundary conditions.—Equations [1]-[3] can be simplified by replacing the instantaneous field with its time average $<E>$. Taking into account Eq. [10] and that

$$<E> = -\frac{dV}{dx} \qquad [18]$$

yields

$$\frac{d}{dx}(n_i u_i) = 0 \qquad [19]$$

$$u_i \frac{du_i}{dx} \doteq -\frac{q}{m}\frac{dV}{dx} - \frac{\alpha_i u_i^2}{m} \qquad [20]$$

$$\frac{d^2V}{dx^2} = -\frac{qn_i}{\epsilon_0} \qquad [21]$$

It now remains to impose suitable boundary conditions on this system of equations. Bohm (27) demonstrated that ions entering the sheath must do so with an approximate velocity which is determined by the plasma parameters characteristic of the glow. If one defines the coordinate origin, $x = 0$, to be at the sheath-glow interface (Fig. 2), the Bohm criterion in a collisionless plasma is

$$u_i(0) \simeq \sqrt{\frac{kT_e}{m}} \qquad [22]$$

Here, T_e is the electron temperature within the glow region. Typically, in an RF discharge of practical importance, kT_e is from 1 to 10 eV.

The essence of the Bohm criterion is that before entering the sheath, an ion falls through a potential drop of order, $kT_e/2q$, which "leaks" into the glow from the sheath. A potential drop of this magnitude can be sustained within the glow due to the thermal energy of the electron fluid without grossly perturbing the system away from ideality (*i.e.*, the glow remains quasi-neutral with approximately equal ion and electron densities). The Bohm criterion must be modified when the negative ion density in the glow is large as compared to the electron density (15).

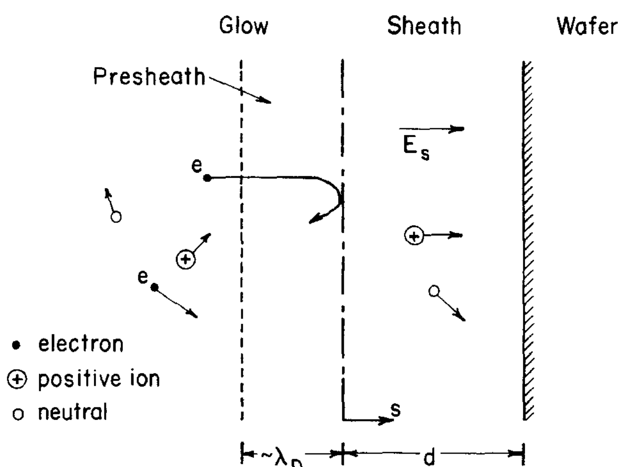

Fig. 2. Schematic of sheath and of sheath/glow interface (not drawn to scale).

If one adopts the convention that $x < 0$ corresponds to the glow and $x > 0$ corresponds to the sheath (and/or electrode), one can modify the Bohm criterion to include the effect of dynamic friction as follows

$$\frac{mu_i(0)^2}{2} \simeq \frac{kT_e}{2} - \int_{-\infty}^{0} dx\,|F_i(x)| \qquad [23]$$

Thus, the kinetic energy of an ion entering the sheath approximately equals the potential energy, $kT_e/2$, minus energy lost to friction against the medium. In practice, the quadrature cannot be evaluated and will be replaced by an estimate, $\lambda_D|F_i(0)|$, where λ_D is the Debye length. The Debye length is a characteristic measure of the distance within a quasi-neutral plasma over which a variation in potential of order, $kT_e/2q$, is effectively screened out. Consequently, electric fields within the plasma should be no greater than the order of $kT_e/2q\lambda_D$. Hence, before entering the sheath, an ion is strongly affected by electrical and frictional forces primarily within the last Debye length of the glow (presheath in Fig. 2) before reaching the sheath-glow interface. Since the average electron energy in the glow associated with the x-degree of freedom is $kT_e/2q$, the sheath-glow interface is the plane at which the average electron is reflected back to the glow, leaving the sheath devoid of electrons, as assumed earlier.

It should be mentioned at this point that the above discussion associated with the Bohm criterion is most appropriate for a dc sheath. For example, periodic electron "leakage" into an RF sheath, to neutralize the positive ion flux to a capacitively coupled electrode, would violate our assumption of the sheath being devoid of electrons. However, it was felt that, for the present simplified sheath model, the Bohm criterion may be used [as was done in previous work on RF sheaths, Ref. (22)] to provide an approximate boundary condition for the ion current at the glow/sheath interface. The problem of suitable boundary conditions at the (imaginary) glow/sheath interface arises when the sheath is considered separately from the glow. Such a problem would not exist in a glow discharge model which is written over the entire interelectrode space (26). However, such a model is far more complex and does not serve the purpose of the present work; namely, to provide a simplified, yet reasonable sheath model which can be readily coupled to a transport and chemical reaction model of a plasma etching reactor.

In the present work, the bulk ion density n_p was taken to be constant within the glow up to the glow-sheath interface ($x = 0$). Thus, the Bohm criterion and quasi-neutrality provide the following boundary conditions at the sheath-glow interface

$$n_i(0) = n_p \qquad [24]$$

$$u_i(0) = \sqrt{\frac{kT_e}{m + 2\alpha_i\lambda_D}} \qquad [25]$$

$$\left.\frac{dV}{dx}\right|_{x=0} = -\frac{kT_e}{2q\lambda_D} \qquad [26]$$

$V(0)$ can be chosen arbitrarily and will be taken to be zero. The electrode is assumed to be an equipotential surface

$$V(d) = -V_s \qquad [27]$$

Equation [27] implies that the electrode has a negative potential with respect to the plasma. The three boundary conditions imposed on potential do not overspecify the problem since the sheath thickness d is not known *a priori*.

It is instructive to render the equations and boundary conditions dimensionless. By defining

$$n_i^* = \frac{n_i}{n_p} \qquad u_i^* = u_i\sqrt{\frac{m}{kT_e}} \qquad V^* = \frac{qV}{kT_e} \qquad [28]$$

$$x^* = \frac{x}{\lambda_D} \qquad \mathrm{Co} = \frac{\alpha_i \lambda_D}{m} \qquad [29]$$

one can rewrite Eq. [19]-[21] to obtain

$$\frac{d}{dx^*}(n_i^* u_i^*) = 0 \qquad [30]$$

$$u_i^* \frac{du_i^*}{dx^*} = -\frac{dV^*}{dx^*} - \mathrm{Co}\, u_i^{*2} \qquad [31]$$

$$\frac{d^2V^*}{dx^{*2}} = -n_i^* \qquad [32]$$

In rendering Eq. [21] dimensionless, the expression for the Debye length $\lambda_D = (kT_e\epsilon_o/n_eq^2)^{1/2}$ was used. The preceding boundary conditions become

$$n_i^*(0) = 1 \qquad u_i^*(0) = \sqrt{\frac{1}{1 + 2\mathrm{Co}}} \qquad [33]$$

$$\left.\frac{dV^*}{dx^*}\right|_{x^*=0} = -\frac{1}{2} \qquad V^*(0) = 0 \qquad V^*(d^*) = -V_s^* \qquad [34]$$

The dimensionless quantity Co, hereafter referred to as the "collision number," directly affects the energy of ions bombarding the electrode. With use of Eq. [17] and [29], Co can be expressed as

$$\mathrm{Co} = \frac{1}{2} N\lambda_D\sigma_t \qquad [35]$$

Co is a measure of the number of collisions an ion suffers when traversing the sheath. If the value of Co is small (Co $\rightarrow$ 0), such as under low pressure operation, ions free-fall into the sheath. This is the so-called space charge sheath limit. In such a case ions bombard the electrode surface with energy equal to the average sheath voltage. At the other extreme of high Co values, ions experience many collisions during their transit through the sheath and ions can be regarded in "equilibrium" with the local field. In that case, ion inertia effects can be neglected ($du_i/dx \simeq 0$), and the ion bombardment energy will be substantially smaller than the sheath voltage.

Combining Eq. [30]-[32] yields

$$\frac{d^2}{dx^{*2}}(u_i^{*2}) + 2\mathrm{Co}\frac{d}{dx^*}(u_i^{*2}) = \frac{2}{u_i^*}\sqrt{\frac{1}{1 + 2\mathrm{Co}}} \qquad [36]$$

which was solved for u_i^{*2} by a finite difference algorithm. Equation [33] provided $u_i^{*2}(0)$, one of the two initial conditions required. The second initial condition was found by applying Eq. [31] for $x^* = 0$, and using Eq. [33] and [34] to obtain

$$\left.\frac{du_i^{*2}}{dx^*}\right|_{x^*=0} = 1/(1 + 2\mathrm{Co}) \qquad [37]$$

After obtaining the drift velocity $u_i^* = u_i^*(x^*)$, Eq. [30] and [32] were solved simultaneously to find the potential distribution in the sheath. Calculations stopped when the potential attained a value of $-V_s^*$, i.e., when the electrode was reached, at which point the sheath thickness could be obtained from the corresponding x^* value.

Results and Discussion

Two sets of calculations were carried out, the first being of general behavior in dimensionless parameter space, the second being specific to an oxygen plasma in a parallel plate etching reactor.

Figure 3 shows the dimensionless sheath potential as a function of dimensionless distance from the glow/sheath interface ($x^* = 0$) into the sheath, for several values of Co. The absolute value of the sheath potential increases monotonically with distance into the sheath. For a given distance into the sheath, the potential "drop" is higher for higher values of the collision number. This is because the sheath "resistance" increases with Co. In practice, if one has an estimate of the sheath voltage and of Co, one can obtain x^* from Fig. 3 and in turn the sheath thickness. For example, in a symmetric discharge (electrode area ratio $\approx$ 1), the sheath voltage may be taken as approximately 1/4 of the applied RF peak-to-peak voltage (assuming that there is negligible voltage drop across the bulk plasma). In a strongly asymmetric system (electrode area ratio << 1), the sheath voltage over the smaller area electrode (usually the powered electrode) may be taken as 1/2 of the applied RF peak-to-peak voltage (11). The collision number is given by Eq. [35] and requires knowledge of the collision cross section, values of which may be found in Ref. (14) and (16).

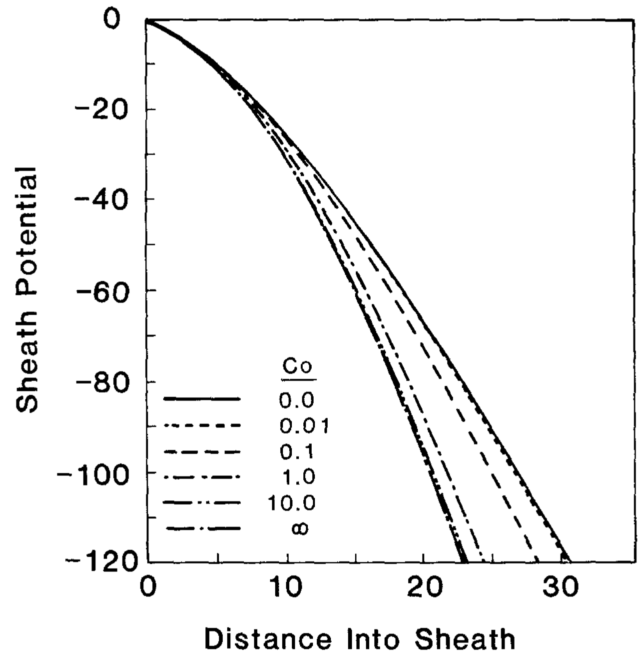

Fig. 3. Dimensionless sheath potential vs. dimensionless distance into the sheath with the collision number as a parameter.

The value of x^* obtained in the foregoing manner can then be used with Fig. 4 to obtain the ion velocity (and energy) for the given Co. As seen in Fig. 4, the ion velocity decreases with increasing Co because ions experience more collisions in the sheath. The ion velocity changes rapidly close to the glow/sheath interface. The current continuity equation then requires that the ion density falls rapidly there. For values of Co > 1, the ion velocity quickly attains a "fully developed" value, changing only slowly with distance down the sheath. This is the force balance condition for which the electrostatic force and the frictional force almost balance each other, *i.e.*, ion inertia (acceleration) is negligible ($du_i/dx = 0$ in Eq. [20]). Then, Eq. [20] yields

$$u_i = \left(\frac{qE}{\alpha_i}\right)^{1/2} \qquad [38]$$

or, since α_i is proportional to pressure p (Eq. [17])

$$u_i \sim \left(\frac{E}{p}\right)^{1/2} \qquad [39]$$

This result was obtained by Wannier (12) for the motion of gaseous ions with fully developed velocity distribution under a strong electric field ($E/p >> 1$ V/torr-cm), and constant mean free path ion-neutral collisions (such as in the case of hard-sphere interactions).

There are some limiting forms of the sheath model which are amenable to analytical solution. In the "frictionless" case (Co $\rightarrow$ 0), Eq. [36] can be solved analytically to

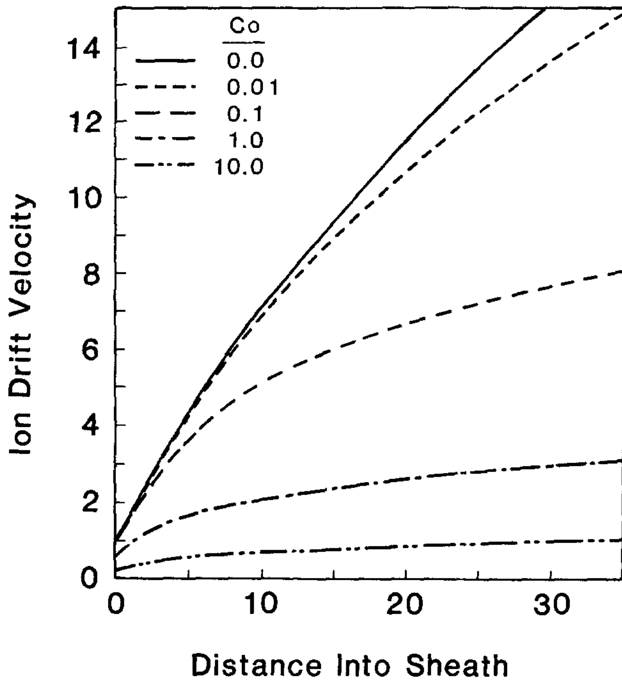

Fig. 4. Dimensionless ion drift velocity *vs.* dimensionless distance into the sheath with the collision number as a parameter.

obtain an explicit expression of ion velocity *vs.* distance into the sheath

$$u_i^* = \left[4y + \frac{585}{512} + z\right]^{1/3} + \left[4y + \frac{585}{512} - z\right]^{1/3} - \frac{7}{8} \quad [40]$$

with

$$y = \frac{9x^{*2}}{16} + \frac{33x^*}{64} \quad [41]$$

and

$$z = 3\left(x^* + \frac{11}{24}\right)\sqrt{y + \frac{29}{64}} \quad [42]$$

For large x^*, the terms containing x^{*2} dominate and Eq. [40] is simplified to

$$u_i^* \approx \left(\frac{9}{2}\right)^{1/3} (x^*)^{2/3} \quad [43]$$

Furthermore, in the frictionless case $u_i^* = \sqrt{1 - V^*}$. For large x^*, for which [43] is valid, $-V^* >> 1$ (recall that $V^* < 0$), and

$$u_i^* \approx \sqrt{-V^*} \quad [44]$$

Noting that $I_+ = qn_iu_i$, taking into account Eq. [44], and introducing dimensional variables into Eq. [43], results in the high vacuum version of the Child-Langmuir law

$$I_+ = \frac{4\epsilon_o}{9}\left(\frac{2q}{m}\right)^{1/2} \frac{V_s^{3/2}}{d^2} \quad [45]$$

Another limiting case results when electrostatic and frictional forces balance each other, *i.e.*, when ion inertia can be neglected. For any finite value of Co, this will happen at sufficiently large x^*. The higher the value of Co, the sooner the ion will attain the force balance condition.

When ion inertia is neglected, the sheath equations can be integrated directly to yield

$$u_i^* = \left(\frac{3}{2\text{Co}\sqrt{1 + 2\text{Co}}}\right)^{1/3} (x^* + C)^{1/3} \quad [46]$$

The integration constant C can be eliminated by using boundary condition Eq. [33]. Then

$$C = \left[\frac{2\text{Co}}{3(1 + 2\text{Co})}\right]^{1/3} \quad [47]$$

However for the large x^* for which Eq. [46] is valid, C can be neglected compared to x^*, and Eq. [46] reduces to

$$u_i^* = \left(\frac{3}{2\text{Co}\sqrt{1 + 2\text{Co}}}\right)^{1/3} (x^*)^{1/3} \quad [48]$$

In addition, integration of Poisson's equation yields for the case at hand (and for high x^*)

$$V^* = -\frac{9}{10}\left[\frac{2\text{Co}}{3(1 + 2\text{Co})}\right]^{1/3} (x^* + C)^{5/3} \quad [49]$$

Equation [48] and [49] indicate that for any finite value of Co, u_i will become asymptotic to a one-third power law and V will become asymptotic to a five-thirds power law with respect to x^*, as $x^* \to \infty$. The above limiting cases are displayed in Fig. 5 where the complete solution (solid lines) is compared to the asymptotic solutions. If Co = 0, the complete solution almost coincides with the Child-Langmuir law, Eq. [43] (dash-dotted line). For Co ≈ 1, the complete solution is virtually identical to the approximate solution Eq. [48]. In fact, for x^* greater than about 10, Eq. [48] is a good approximation for values of Co ≳ 0.1.

Consider now the range of values of Co that would be encountered in practice. For O_2^+ moving in its parent gas, for example, the total collision cross section has been reported as $\sigma_t = 5.5\ 10^{-15}$ cm^2 (16). For Cl_2^+ in Cl_2, $\sigma_t = 2.67\ 10^{-15}$ cm^2 (14). Therefore a typical value of σ_t may be taken as $5\ 10^{-15}$ cm^2. For a high pressure plasma etching reactor for which $p = 0.5$ torr and $T = 350$ K, the gas density is $N = 1.38\ 10^{16}$ cm^{-3}; a typical value of λ_D is 100 μm or 10^{-2} cm. Then Eq. [35] yields Co ≈ 0.5. Further, a typical sheath thickness is a few mm, *i.e.*, x^* is a few decades. As shown above, under these conditions, Eq. [48] and [49] are good

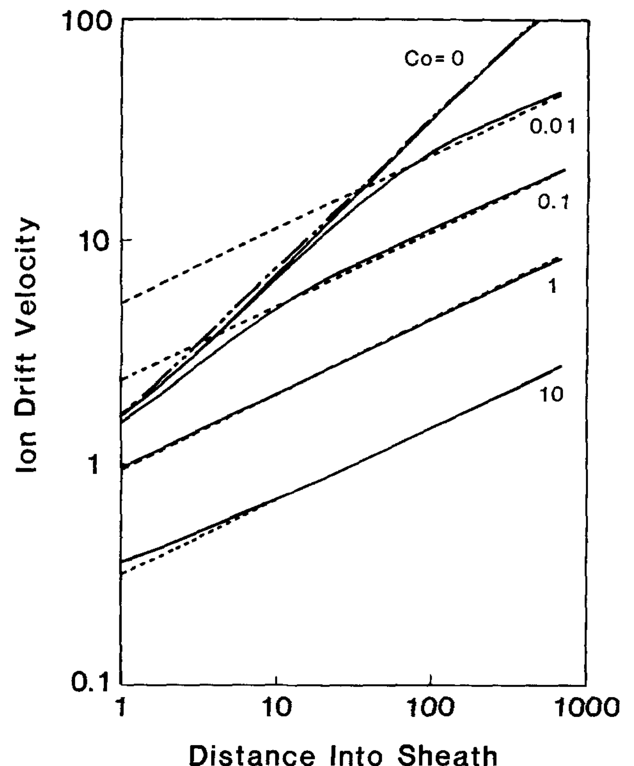

Fig. 5. Dimensionless ion drift velocity *vs.* dimensionless distance into the sheath with the collision number as a parameter. ———, Numerical solution to Eq. [36]; —·—·—, analytic expression Eq. [43]; - - - -, analytic expression Eq. [48].

approximations. Then, by eliminating ($x^* + C$) between these two equations, one has an expression for the ion bombardment energy as a function of the sheath voltage, applicable to relatively high pressure plasma etching reactors

$$(u_i^*)^2 = \frac{(-10V^*)^{2/5}}{(2Co)^{4/5}(1 + 2Co)^{1/5}} \quad [50]$$

Equation [50] provides the dimensionless ion energy as a function of the dimensionless potential down the sheath (V^*), for relatively high values of Co. The ion bombardment energy can be obtained when the sheath voltage (V_s^*) is used for V^*. As an example, consider a sheath voltage $V_s = -250$V and a plasma electron temperature $T_e = 4$ eV. Then $V_s^* = -250/4 = -62.5$. Assuming Co = 0.5, as calculated above, one finds $(u_i^*)^2 = 11.4$ and the ion kinetic energy $\epsilon_i = 1/2\ mu_i^2 = 11.4 \cdot 2 = 22.8$ eV. This would be the energy in ordered motion. The total ion bombardment energy would be $\epsilon_+ = 22.8/0.559 = 40.8$ eV (see Eq. [52] below).

Besides considering the general characteristics of the sheath, the model was also applied to an actual plasma etching reactor. The experimental system has been described elsewhere (13). Briefly, an oxygen discharge was used to etch polymeric films in a showerhead parallel plate single-wafer etcher. The substrate wafer was resting on the grounded electrode. The average plasma (and ground sheath) potential ($\mathbf{V}_p$) was estimated from measurements of the RF peak-to-peak applied voltage (V_{pp}) and of the dc self-bias (V_{dc}) with the equation $\mathbf{V}_p = (V_{pp}/2 + V_{dc})/2$ (11). The dc bias was small in the approximately symmetric sys tem used. The above equation for $\mathbf{V}_p$ is not applicable when a substantial voltage drop occurs across the bulk plasma, such as under conditions resulting in low electron mobility and/or density. However under typical conditions (~1 torr, 100W) it was found that the plasma resistance (~10Ω) was small compared to the sheath impedance (~150Ω) suggesting that the voltage drop across the bulk plasma was typically small. The average electron density and temperature were found as described in Ref. (13). The purpose was to calculate the energy and flux of ions bombarding the substrate electrode as a function of reactor operating pressure and power input. These quantities have direct bearing on the etching rate and the degree of anisotropy of films.

Oxygen discharges are known to be electronegative, *i.e.*, the negative ion density can exceed the electron density. However, for a pressure of 1 torr, Dettmer (23) found that the density of the dominant negative ion (O^-) in a dc oxygen discharge became small, compared to the electron (and positive ion) density, for reduced electric fields in the bulk plasma $E_b/N \gtrsim 55$ *Td* (1 *Td* = 10^{-17} V-cm^2). The reduced effective electric field (24) E_{ef}/N in the bulk plasma was calculated to be typically above 50 *Td* in the system studied. Under the assumption that a high frequency (and relatively high pressure) RF discharge of a given E_{ef}/N is comparable to a dc discharge with the same E_b/N, the negative ion concentration may therefore be neglected for the system at hand. However, since the present sheath model pertains to electropositive gases, application of the model to an oxygen discharge should be limited to conditions under which the negative ion density is low.

The ion kinetic energy owing to the drift velocity is $\epsilon_i = 1/2\ mu_i^2$. By defining a dimensionless ion energy $\epsilon_i^* = 2\epsilon_i/kT_e$ one finds by using u_i^* from Eq. [28]

$$\epsilon_i^* = (u_i^*)^2 \quad [51]$$

This is the ion energy in ordered motion (associated with the ion drift velocity). However the total ion energy is higher since ions also have a random velocity component. It is the total ion energy which affects the etching kinetics. For the constant mean free path case considered here, Wannier (12) obtained a relationship between the ion kinetic energy in ordered motion and the total average ion kinetic energy, which can be expressed here as

$$\epsilon_+^* = \epsilon_i^*/0.559 \quad [52]$$

One notes that a significant fraction of the total ion energy is associated with random motion. Equation [52] holds in the high pressure regime where the ionic mean free path is much less than the sheath thickness, so that the ion velocity distribution function is well developed. Use of Eq. [52] under low pressure conditions will overestimate the total ion energy. The dimensionless ion flux is

$$I_+^* = u_i^* n_i^* = 1/\sqrt{1 + 2Co} \quad [53]$$

Quantities such as ϵ_+^* and I_+^* can be used in models for the ion-assisted kinetics to predict the ion-assisted etching rate. This can in turn be used in transport models of plasma reactors (13).

Figure 6 shows the dependence of ion bombardment energy on reactor pressure for different values of power input. Ion energies are indeed low. This is a result of the combination of low sheath voltages (~200V) and many ion collisions in the sheath, at the relatively high pressures used. The situation may be drastically different in low pressure (~10 mtorr) reactive ion etching reactors with the wafer resting on the (high sheath voltage) smaller size electrode. Ion energies as high as 500 eV are easily obtainable in such systems. For a given power, ion energy decreases monotonically with pressure due to increased number of collisions and lowered sheath electric field. The decrease in energy with pressure may be partly counterbalanced by increasing the power input.

The variation of ion flux with pressure is shown in Fig. 7. The behavior can be explained by introducing dimensional variables into Eq. [53] to obtain

$$I_+ = n_p \left(\frac{kT_e/m}{1 + 2Co}\right)^{1/2} \quad [54]$$

The decrease of I_+ with pressure is the result of T_e and n_p decreasing, and of Co increasing with pressure (note that n_p increases with pressure at low pressures, ≲0.2 torr in our case, but decreases at high pressures). The decrease of I_+ is sharper at lower pressures mainly because n_p shows similar behavior with pressure (13). For constant pressure, ion flux increases almost linearly with increasing power. This is because n_p increases linearly with power and the term in parenthesis in Eq. [54] is only weakly dependent on power. Ion flux is independent of sheath voltage for a sourceless sheath. This would not be the case if ionization occurred in the sheath by secondary electrons, for example. Such electrons are emitted from the electrode by the bombarding ions and are accelerated by the sheath electric field back into the glow. When pressure is high, secondary electrons can cause ionization in the sheath (10). This re-

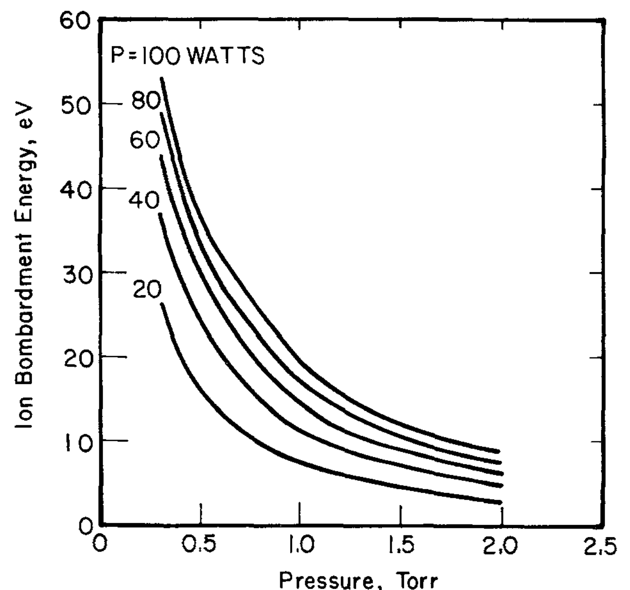

Fig. 6. Ion bombardment energy vs. reactor pressure with power as a parameter.

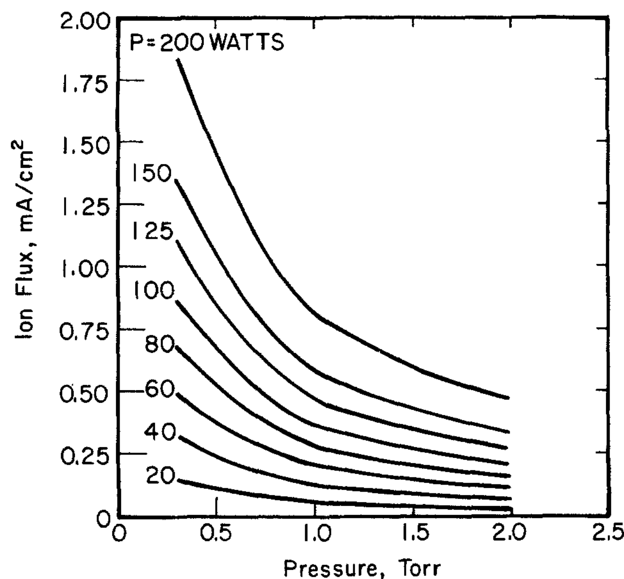

Fig. 7. Ion bombardment flux vs. reactor pressure with power as a parameter.

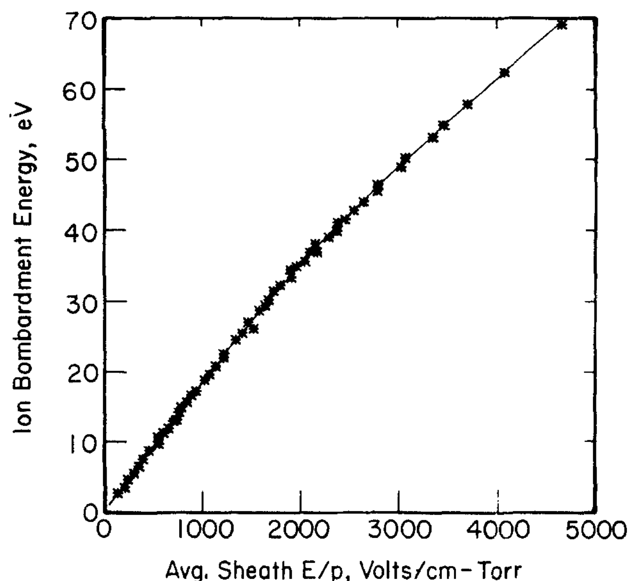

Fig. 8. Ion bombardment energy vs. average sheath-electric-field-to-pressure ratio.

sults in higher ion current to the substrate and to thinner sheath as compared to the sourceless sheath case. When ionization in the sheath by secondary electrons takes place, the ion flux on the substrate electrode is

$$I_+ = \frac{I_{+0}}{1 - \gamma_i[\exp(N\sigma_i d) - 1]} \quad [55]$$

where I_{+0} is the ion current injected into the sheath at the glow/sheath interface. The maximum ionization cross section for electrons in oxygen, for example, is $\sigma_i = 2.72\ 10^{-16}$ cm^2 (16). As previously, one may take neutral density $N = 1.38\ 10^{16}\ cm^{-3}$ (0.5 torr, 350 K) and $d \simeq 0.1$ cm. For the ion energies of interest, the secondary electron emission coefficient has a value of ≤ 0.1 for many electrode materials under noble ion bombardment, and is usually much smaller for molecular ion bombardment (11, 16). Then, for $\gamma = 0.1$, the denominator in Eq. [55] is about 0.95, which amounts to a 5% increase in current due to ionization in the sheath, under the above conditions. This is rather an upper limit on the expected degree of ionization by secondary electrons under these conditions. Similarly, ion-impact ionization may also be neglected. For example, using the rather high value of $\sigma_i = 10^{-16}$ cm^2 for the corresponding cross section and values of N and d as above, one obtains an ion multiplication factor of $\exp(N\sigma_i d) = 1.14$ ions produced per ion. Again, this is an overestimate of the ionization in the sheath, under the above conditions.

The dependence of ion energy on the sheath electric-field-to-pressure ratio, E_s/p, has been recognized in the literature (1, 2, 12). In order to investigate further that relationship, E_s/p and ion energy (Eq. [52]) were calculated for different values of pressure and power in the range 0.3-2 torr and 20-200W, respectively. For each pressure-power pair the average sheath electric field was found by integrating the computed electric field distribution over the sheath thickness. The results are shown in Fig. 8. One observes that there exists a unique functional relation between ion bombardment energy and sheath E_s/p. Low values of E_s/p occur at higher pressure (high Co). Under these conditions electrostatic and frictional forces balance each other, and Eq. [39] is applicable. Hence ion energy is linear in E_s/p. At high E_s/p (low pressure), ion inertia is not negligible and the data deviate from the straight line passing through the origin. The deviation is negative because $u_i\ du_i/dx$ is positive, *i.e.* the ion velocity has not had a chance to achieve its "fully developed" value (ions strike the electrode before that happens).

No experimental data on ion bombardment energy and flux in oxygen plasma etching reactors could be found in the literature to test the predictions of the sheath model. Thompson *et al.* (1, 25), and Allen *et al.* (17) used a similar reactor system to that employed in the present study. Their experimental conditions were mostly within the range covered in the present work, except that the authors used gases such as CF_3Cl, CF_3Br, and SF_6. Values of the measured ion bombardment energy and ion flux were similar to the values shown in Fig. 6 and 7, although such similarity may be fortuitous. The variation of ion bombardment energy with power and pressure was also similar to that predicted by the present sheath model. Ion bombardment energy and flux critically affect etch anisotropy in plasma-assisted etching applications. A realistic plasma reactor model must provide for the calculation of these quantities.

Summary and Conclusions

An approximate model of the RF plasma sheath was developed. The ion drift velocity was found by coupling the ion "fluid" equations to Poissons' equation for the potential distribution in the sheath. Ion-neutral collisions were accounted for by a frictional force opposing the ion motion. An analysis of the collision dynamics showed that, for ion energies much greater than the background medium thermal energy, the frictional force may be taken proportional to the square of the ion velocity. The proportionality constant increases linearly with the collision cross section and with pressure. The dimensionless number Co (Eq. [35]) was found to be important in describing the sheath properties. Typical values of Co in high pressure (~1 torr) plasma etching reactors are around unity. For such values of Co, frictional and electrostatic forces on the ion quickly balance each other. An analytic solution was then derived yielding the ion bombardment energy as a function of the sheath potential. Such expression may be used for quick estimation of expected ion energy in high pressure plasma etching reactors. At the extreme of no collisions in the sheath (Co → 0) the Child-Langmuir law was recovered.

The model was applied to a high pressure parallel plate plasma reactor used to etch polymer films in an oxygen discharge. The energy of ions bombarding the grounded electrode was calculated to be only a few tens of eV, much lower than typical sheath voltages (~200V). Ion energy and ion flux decreased with pressure and increased with power. Over the range of variables investigated, the ion bombardment energy was found to be a unique function of the average sheath electric-field-to-pressure ratio, E_s/p. In fact, ion energy was linear with E_s/p for values below about 2000 V/cm-torr, but deviated from linearity for higher E_s/p values.

The assumptions introduced in the model limit the parameter range over which the model is applicable. For ex-

ample, a time dependent phenomena (18, 19) must be incorporated for frequencies below 5 MHz (30). Ionization in the sheath may become important for pressures higher than about 1 torr (10). Finally, only the average ion energy and not the ion energy distribution (8, 20) can be found. Nevertheless, the simplified sheath model developed here can be readily coupled to a more general plasma etching reactor model, including transport and reaction phenomena of the etching species, to calculate etch rate, uniformity, and anistropy of etching thin films (13). The present sheath model may also be used to construct equivalent electrical circuits of the sheath (21, 22). For example, the model allows one to relate molecular quantities, such as collision cross sections, to equivalent circuit components, such as sheath resistance and capacitance.

Manuscript submitted March 26, 1987; revised manuscript received Aug. 28, 1987.

The University of Illinois assisted in meeting the publication costs of this article.

LIST OF SYMBOLS

Co collision number, Eq. [35], dimensionless
d sheath thickness, cm
D collision diameter, cm
E sheath electric field, V/cm
erf error function
F_i frictional force on ion, dynes
$\mathbf{g}$ relative velocity of test ion with respect to neutral molecule, cm/s ($g = |\mathbf{g}|$)
I_+ ion current, mA/cm^2
k Boltzmann's constant, 1.38 10^{-23} J/K
m particle mass, g
N neutral particle density, cm^{-3}
n charged particle density, cm^{-3}
p pressure, torr
q fundamental charge, 1.609 10^{-19} Cb
T temperature, K
t time, s
u_i ion velocity, cm/s
V potential, V
v neutral particle velocity, cm/s
x x-coordinate, cm

Greek characters

α_i proportionality factor in Eq. [10], g/cm
γ_i secondary electron emission coefficient, dimensionless
ϵ_i ion energy in ordered motion, ergs or eV
ϵ_+ total ion energy, ergs or eV
ϵ_o permittivity of the free space, 8.85 10^{-14} F/cm
θ angle between $\mathbf{g}$ and X-axis, degrees
λ_D Debye length, cm
σ collision cross section, cm^2
χ scattering angle, degrees

Subscripts

e electron
el elastic collision
ex charge exchange collision
i ions, ionization
p plasma
s sheath
t total

Superscript

* dimensionless quantity

REFERENCES

1. B. E. Thompson, K. D. Allen, A. D. Richards, and H. H. Sawin, *J. Appl. Phys.*, **59** (6), 1890 (1986).
2. C. B. Zarowin, *J. Vac. Sci. Technol.*, **A2** (4), 1537 (1984).
3. V. M. Donnelly, D. L. Flamm, and R. H. Bruce, *J. Appl. Phys.*, **58** (6), 2135 (1985).
4. R. H. Bruce and A. R. Reinberg, *This Journal*, **129** (2), 393 (1982).
5. D. J. Economou and R. C. Alkire, Submitted to *This Journal.*
6. R. H. Bruce, *J. Appl. Phys.*, **52** (12), 7064 (1981).
7. K. Kohler, J. W. Coburn, D. E. Horne, E. Kay, and J. H. Keller, *ibid.*, **57** (1), 59 (1985).
8. I. Abril, A. Gras-Marti, and J. A. Valles-Abarca, *J. Vac. Sci. Technol.*, **A4** (3), 1773 (1986).
9. M. J. Kushner, *J. Appl. Phys.*, **58** (11), 4024 (1985).
10. W. B. Pennebaker, *IBM J. Res. Develop.*, **23** (1), 16 (1979).
11. B. Chapman, "Glow Discharge Processes: Sputtering and Plasma Etching," John Wiley and Sons, Inc., New York (1980).
12. G. H. Wannier, *Bell System Tech. J.*, **32,** 170 (1953).
13. D. J. Economou and R. C. Alkire, Submitted to *AIChE J.*
14. E. W. McDaniel and E. A. Mason, "The Mobility and Diffusion of Ions in Gases," John Wiley and Sons, Inc., New York (1973).
15. R. L. F. Boyd and J. B. Thompson, *Proc. R. Soc. London, Ser. A*, 102 (1959).
16. E. W. McDaniel, "Collision Phenomena in Ionized Gases," John Wiley and Sons, Inc., New York (1964).
17. K. D. Allen, H. H. Sawin, M. T. Mocella, and M. W. Jenkins, *This Journal*, **133,** 2315 (1986); K. D. Allen and H. H. Sawin, *ibid.*, **133,** 2326 (1986); K. D. Allen, H. H. Sawin, and A. Yokozeki, *ibid.*, **133,** 2331 (1986).
18. R. T. C. Tsui, *Phys. Rev.*, **168** (1), 107 (1968).
19. R. A. Gottscho, *Mat. Res. Soc. Symp. Proc.*, **38,** 55 (1985).
20. W. D. Davis and T. A. Vanderslice, *Phys. Rev.*, **131** (1), 219 (1963).
21. A. Metze, D. W. Ernie, and H. J. Oskam, *J. Appl. Phys.*, **60** (9), 3081 (1986).
22. C. M. Horwitz, *J. Vac. Sci. Technol.*, **A1** (1), 60 (1983).
23. J. W. Dettmer, Ph.D. Thesis, AFIT/DS/78-3, Air Force Institute of Technology (1978).
24. B. E. Cherrington, "Gaseous Electronics and Gas Lasers," Pergamon Press, New York (1980).
25. B. E. Thompson and H. H. Sawin, *This Journal*, **133** (9), 1887 (1986).
26. D. B. Graves and K. F. Jensen, *IEEE Trans. Plasma Sci.*, **PS-14** (2), 78 (1986).
27. D. Bohm, in "The Characteristics of Electrical Discharges in Magnetic Fields," A. Guthrie and R. K. Wakerling, Editors, McGraw-Hill, Inc., New York (1949).